

## Research



**Cite this article:** Deck S, Gand F, Brunet V, Ben Khelil S. 2014 High-fidelity simulations of unsteady civil aircraft aerodynamics: stakes and perspectives. Application of zonal detached eddy simulation. *Phil. Trans. R. Soc. A* **372**: 20130325.  
<http://dx.doi.org/10.1098/rsta.2013.0325>

One contribution of 13 to a Theme Issue 'Aerodynamics, computers and the environment'.

**Subject Areas:**  
fluid mechanics

**Keywords:**  
large eddy simulation, aerodynamics, computational fluid dynamics, turbulence modelling

**Author for correspondence:**  
Sébastien Deck  
e-mail: [sebastien.deck@onera.fr](mailto:sebastien.deck@onera.fr)

# High-fidelity simulations of unsteady civil aircraft aerodynamics: stakes and perspectives. Application of zonal detached eddy simulation

Sébastien Deck, Fabien Gand, Vincent Brunet and Saloua Ben Khelil

ONERA—The French Aerospace Laboratory, 92190 Meudon, France

This paper provides an up-to-date survey of the use of zonal detached eddy simulations (ZDES) for unsteady civil aircraft applications as a reflection on the stakes and perspectives of the use of hybrid methods in the framework of industrial aerodynamics. The issue of zonal or non-zonal treatment of turbulent flows for engineering applications is discussed. The ZDES method used in this article and based on a fluid problem-dependent zonalization is briefly presented. Some recent landmark achievements for conditions all over the flight envelope are presented, including low-speed (aeroacoustics of high-lift devices and landing gear), cruising (engine–airframe interactions), propulsive jets and off-design (transonic buffet and dive manoeuvres) applications. The implications of such results and remaining challenges in a more global framework are further discussed.

## 1. Introduction

Simulation tools play an increasingly important role in aeronautics owing to highly innovative technologies and complex systems needed to meet high safety requirements and sustainable aviation objectives in terms of emissions and noise [1,2]. This challenging yet essential reduction of the environmental impact of aviation involves improvements in air traffic management, systems efficiency, original and optimized configurations, among many other fields. In particular,

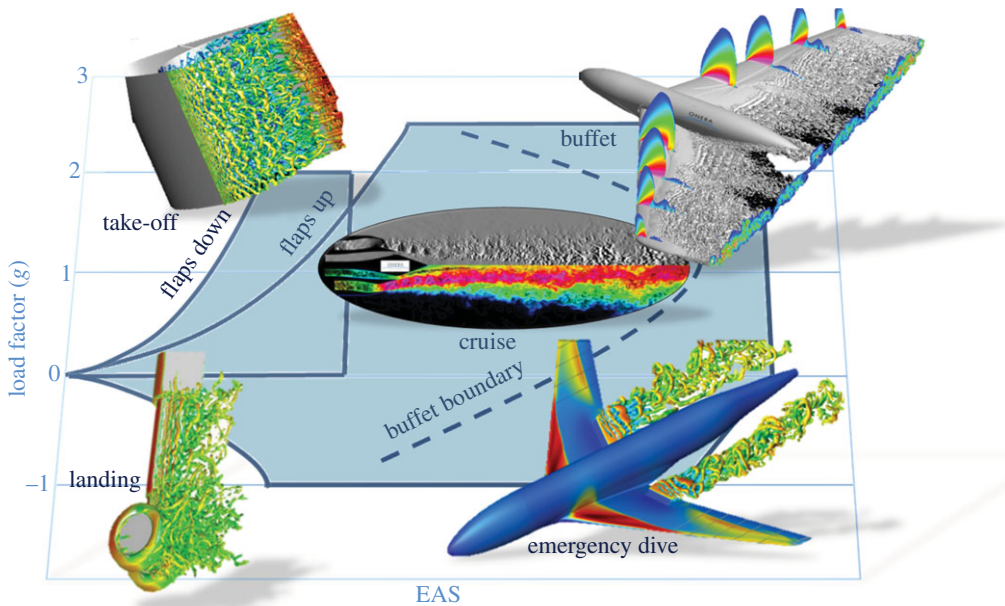


**Figure 1.** Generic flight envelope of a transport civil aircraft (shaded graph area) and illustrations of hybrid simulations at flight conditions for which the level of confidence of standard CFD methods is low. The load factor is the ratio between the lift of the aircraft and its weight. Equivalent air speed,  $EAS = \sqrt{2q/\rho_0}$ , where  $q$  is the dynamic pressure, and  $\rho_0$  is the standard sea-level density. (Online version in colour.)

when it comes to greener aircraft and environment preservation, aerodynamics is involved in two main problematics: designing light-weight aircraft by reducing tolerances, and developing innovative and more efficient solutions. In fact, the creation of highly accurate aerodynamic models as a result of high-fidelity methods will allow designers to reduce safety factors (which are important because current methods are mostly based on empiricisms), and thus to lower aircraft mass and, more generally, to optimize aircraft performance. On the acoustic side, the use of hybrid methods at early design stages should help to reduce the acoustic imprint of the aircraft, owing to a better prediction of the location and intensity of the aeroacoustic sources. All these aspects can benefit from a better understanding of the involved physical mechanisms, leading to a better accuracy of the predicted aerodynamic performance of aircraft, which is the focus of this paper.

As an example, figure 1 depicts the typical flight envelope of a generic civil transport aircraft. The corresponding flow conditions are dominated by turbulence. The capability to simulate accurately the three-dimensional unsteady turbulent flow at certain phases of the flight is becoming an especially pressing issue, because a wide range of unsteady phenomena that have serious implications in terms of achievable performance, acoustic environment or safety have to be considered, and therefore need to be accurately predicted as early as possible in the design cycle of an aircraft [3]. Illustrations of some critical off-design conditions for which standard numerical approaches (e.g. Reynolds-averaged Navier–Stokes, RANS) are not reliable have been added to figure 1. For this type of flow physics, hybrid methods are expected to increase the accuracy of the simulations. One can note that, even in cruise conditions, improvements can be achieved through a better prediction of the interactions between engine jets and the airframe, which is a critical issue in terms of structural design and thermal fatigue.

This article aims at demonstrating the capabilities of advanced turbulence modelling methods to reach high levels of confidence in design and off-design conditions and how these achievements can be favourably considered by aircraft makers. Therefore, §2 is devoted to a quick presentation of current turbulence modelling methodologies. The issue for hybrid RANS–large

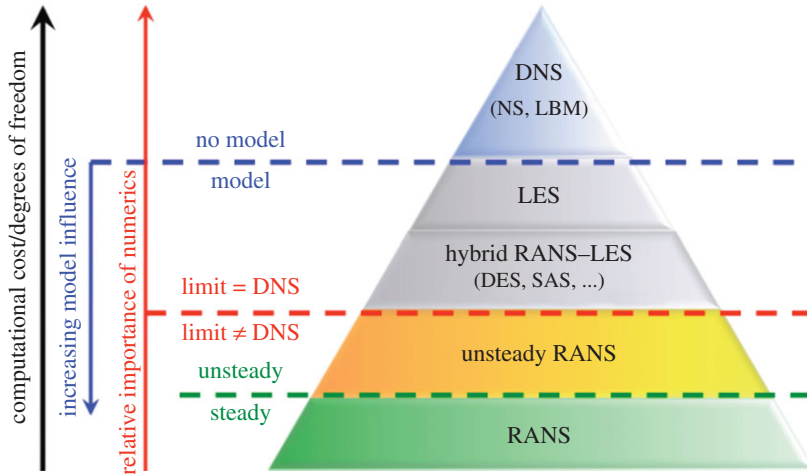


**Figure 2.** Classification of unsteady approaches according to levels of modelling and readiness (adapted from Sagaut *et al.* [8]). (Online version in colour.)

eddy simulation (LES) approaches to the zonal or non-zonal treatment of turbulent flows is also briefly discussed and the salient features of the zonal detached eddy simulation (ZDES) method are presented. Some significant applications for critical flow conditions such as the ones described in figure 1 are presented in §3 of the paper, in order to bring into focus the improvements that can be expected. From these applications, limitations and issues related to the use of such advanced methods are identified and further discussed in §4.

## 2. A glimpse at advanced simulations of unsteady turbulent flows

### (a) Classification of unsteady methods

Current numerical methodologies have to be able to cover a wide range of applications, ranging from external aerodynamics to internal flows. One of the salient features of turbulent flows is their multiscale character, and practical turbulent flows at high Reynolds numbers exhibit such a wide range of excited length and time scales (shock waves, boundary and free shear layers, etc.) that direct numerical simulations (DNS) cannot be envisaged for the foreseeable future. Indeed, let us recall that Moin & Kim [4] reported that, for a civil airliner with a 50 m long fuselage and wings with a chord length of 5 m cruising at  $250 \text{ m s}^{-1}$  at an altitude of 10 km, about  $10^{16}$  points are necessary to simulate the turbulence near the surface with reasonable details. They estimate that even with a supercomputer capable of 1 Teraflops, it would take several thousand years to compute each second of flight time! Although very pessimistic, several other estimates applied to aeroplanes confirm that DNS cannot be considered in the near future (see for instance the discussions by Chapman [5], Spalart *et al.* [6] and Choi & Moin [7]).

This amounts to approximating the effects of unrepresented scales. As discussed by Sagaut *et al.* [8], multiscale and multiresolution approaches have attracted enormous recent interest in a variety of scientific disciplines and particularly in computational fluid dynamics (CFD).

The classical approaches used are RANS and LES (see figure 2). However, and though still in high demand, a steady RANS solution which relies on the modelling of all turbulent scales is useless if unsteady separations occur or if aeroacoustic sources have to be finely characterized. Conversely, the ability of the LES technique to correctly simulate the spatio-temporal dynamics of turbulent flows is now well acknowledged. This technique relies on a decomposition of the aerodynamic field between the large scales (responsible for turbulence production) and the small scales of the flow, the former being directly resolved, whereas the

effect of the latter is modelled. The primary obstacle to practical use of LES on industrial flows, which involve wall boundary layers at high Reynolds number, remains computational resources. Indeed, the capture of the scales of motion accountable for turbulence production imposes severe demands on the grid resolution near solid walls because, in the inner layer of the boundary layer, the energy-carrying structures also contribute much to turbulent dissipation, because the scale separation vanishes at the wall. Therefore, the scale separation on which the so-called wall resolved large eddy simulation (WRLES) technique relies is consequently much reduced (see the discussions in [9–11] among others), which increases even more the CPU cost of the technique.

A recent survey by NASA [12] estimates that WRLES for engineering purposes will still be out of reach in 2030 even with leading HPC machines. Furthermore, it can be argued that the simulation of the dynamics of the smaller scales in attached turbulent boundary layers is most often not necessary from an engineering point of view, while the large-scale turbulent processes within separations and free shear layers need to be accurately assessed. For that reason, hybrid RANS–LES methods were developed to alleviate the resolution constraint of WRLES in the near-wall regions and allow an LES-like resolution everywhere else. It is arguably the most promising strategy for making LES affordable at high Reynolds numbers in a wide range of complex industrial applications.

## (b) Discussion on zonal/non-zonal treatment of turbulence

As mentioned above, it is now commonly acknowledged (see Haase *et al.* [13]) that hybrid RANS–LES is the main strategy to drastically reduce computational cost (compared with standard WRLES) in a wide range of complex industrial applications. Despite a large number of approaches (and acronyms!), these methods are close to one another and can often be rewritten as variants of a small group of generic approaches. In practice, these methods differ by their maturity in the sense that many have not been thoroughly validated or widely used on ‘real’ three-dimensional configurations (see the discussions in [8,14]). At the same time, these methods raise the important question whether the treatment of turbulence has to be zonal or not.

In [15], Deck clearly advocates the use of a zonal treatment of turbulence to handle complex configurations, even if the decision load of the user is increased, for several reasons.

First, because hybrid RANS–LES is primarily an LES except on the wall, a ‘black-box push-button’ method, though very tempting, is perhaps not a desirable option. Indeed, the design of the grid for a hybrid RANS–LES calculation is far from trivial. In the framework of a zonal approach, the grid refinement needs to be focused on regions of interest (e.g. LES regions) without corrupting the boundary layer properties farther upstream or downstream. Besides, boundary layer modelling (in a wall modelled large eddy simulation, WMLES, sense) and its different flavours are essential to match the cost of realistic simulations to the capability of the computer systems available nowadays. In the case of a wall turbulence simulation, it has been shown [16] that, without fixing the RANS–LES interface, the error made on Reynolds shear stress and friction coefficient with respect to the RANS solution varies in a non-trivial manner with grid resolution in the wall parallel direction. In other words, the ability of an ‘automatic’ method to simulate accurately wall turbulence on coarse grids has still to be demonstrated.

Second, although an LES resolution is not required for the whole aircraft, it can be foreseen that in the near future the activation of LES in a boundary layer embedded in an industrial configuration will be considered, which points naturally towards a zonal method. Furthermore, such an approach also allows flexibility in the numerics to adapt the numerical accuracy to the physical resolution level.

Finally, it is worth stressing that a zonal approach also permits operation in a non-zonal mode (but the reverse is not true), which can be of use for specific flow problems, as will be highlighted in the next sections.

However, in the frame of a zonal treatment, the practitioner needs best practice guidelines as well as some basic *a priori* knowledge of the flow considered, such as whether it is a free-shear layer type flow, a purely wall-bounded type flow or a mixture of the two. The authors' position is now increasingly shared by other teams [14,17]. As an example, in the framework of turbomachinery applications, Tyacke *et al.* [18] state that 'the expectation of producing a single modelling strategy that will work effectively and reliably for all engine zones is unrealistic'!

The ZDES approach presented in §2c enables one to combine the best features of both zonal and non-zonal approaches in a unified framework in order to provide an efficient RANS–LES methodology for most technical applications.

### (c) Zonal detached eddy simulation

The ZDES was first proposed by Deck [19,20], and the complete formulation that proposes an efficient solution to prevent delay in the formation of instabilities has been recently published in reference [15].

This approach takes full advantage of its zonal nature, not only to allow the user to specify RANS and LES regions, but also to make possible the use of various formulations within the same calculation. Besides, the ZDES also provides an 'automatic' operating option (referred to as mode 2 in the following) for which the switch between RANS and LES regions is dynamically set by the model itself.

Thus, ZDES offers an attractive flexibility in the treatment of turbulent flows in technical applications and has been applied often with good results over a range of Mach numbers and configurations (see [15]). To guide the aerodynamicist through the simulation process, a system based around flow taxonomies is proposed in the framework of ZDES. This suggestion is also highly supported by Tyacke *et al.* [18].

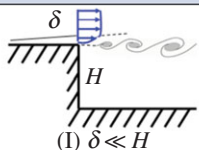
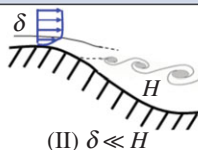
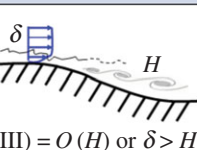
In the framework of ZDES, three specific hybrid length-scale formulations, also called modes, are then optimized to be employed on three typical flow field topologies (figure 3). Mode 1 concerns flows where the separation is triggered by a relatively abrupt variation in the geometry; mode 2 is retained when the location of separation is induced by a pressure gradient on a gently curved surface; and mode 3 is for flows where the separation is strongly influenced by the dynamics of the incoming boundary layer. This latter mode is often referred to as WMLES mode (see [11,16]). The ZDES method aims to treat all classes of flow problems and typical associated applications (indicated in figure 3) in a single model, which defines a hybrid length scale  $\tilde{L}$  that enters any turbulence model (because the eddy viscosity  $\nu_t \approx V \times L$  is the product of a velocity scale  $V$  and a length scale  $L$ ) and reads as

$$\tilde{L}_{\text{ZDES}} = \begin{cases} L_{\text{RANS}} & (\text{mode} = 0), \\ \tilde{L}_{\text{DES}}^{\text{I}}(\tilde{\Delta}) & (\text{mode} = 1), \\ \tilde{L}_{\text{DES}}^{\text{II}}(\tilde{\Delta}) & (\text{mode} = 2), \\ \tilde{L}_{\text{DES}}^{\text{III}}(\tilde{\Delta}) & (\text{mode} = 3), \end{cases} \quad (2.1)$$

where  $\tilde{\Delta}$  is the new subgrid length scale entering  $\tilde{L}_{\text{ZDES}}$ . In the framework of ZDES, the proposal of a new subgrid length scale  $\tilde{\Delta}$  is not a minor adjustment of the detached eddy simulation (DES) formulation, because the modified length scales depend not only on the grid ( $\Delta x, \Delta y, \Delta z$ ), but also on the velocity gradients ( $U_{i,j}$ ) and eddy viscosity fields ( $\nu_t$ ), because

$$\tilde{\Delta} \equiv \tilde{\Delta}(\Delta x, \Delta y, \Delta z, L_{\text{RANS}}, U_{i,j}, \nu_t). \quad (2.2)$$

It is important to stress that with mode 2 of ZDES, which clearly borrows ideas from the delayed detached eddy simulation (DDES) approach [21], it is permitted to operate in an 'automatic' manner, because  $\tilde{L}_{\text{DES}}^{\text{II}}$  uses the same protection function as DDES to maintain the RANS behaviour in the attached boundary layer. Once again, the improvement from the DDES formulation lies in the definition of  $\tilde{\Delta}$  becoming the new subgrid length scale in LES areas, thus

zonal detached eddy simulation (ZDES)			
	mode 1	mode 2	mode 3
flow category			
applications	base flow, free shear flows, spoilers, steps, slat/flap cove, etc.	buffet, flaps, duct flows, nacelle intake, etc.	corner flows, turbulent boundary layer, separation onset on high-lift devices, shallow separations, etc.

**Figure 3.** Classification of typical flow problems, associated ZDES modes and examples of applications. (I) Separation fixed by the geometry; (II) separation induced by a pressure gradient on a curved surface; (III) separation strongly influenced by the dynamics of the incoming boundary layer (adapted from Deck [15]). (Online version in colour.)

taking into account flow parameters (equation (2.2)), whereas the maximum cell size is retained as the subgrid length scale in the DDES ( $\Delta_{\text{DDES}} = \max(\Delta_x, \Delta_y, \Delta_z)$ ). Using equation (2.2) in LES areas for mode 2 solves the problem of delay in the formation of instabilities, which can have dramatic effects on the pressure (and, thus, acoustic) field (see [22]).

### 3. Basic physics investigation of civil aircraft aerodynamics

Spalart & Bogue [23] discussed the long-term ambitions of CFD when applied away from the design point or concept, and therefore in the historically weak areas of CFD. This implies accurately simulating products of the flow such as noise or thermal fatigue as well as undesirable flight conditions, such as transonic buffet and dive conditions. Besides, an accurate prediction of these phenomena is as dependent on the physical understanding of the processes involved and the ideas behind the turbulence treatment as it is on computing power. In this regard, ZDES offers an attractive flexibility in the treatment of turbulent flows in technical applications, because most flow problems fall into the flow taxonomies proposed in figure 3. To give an idea of the current status of the method and its maturity towards its use in an industrial context, several critical conditions (as displayed in figure 1) have been selected and presented in the following. Most computations have been performed with the elsA software [24], which solves the compressible Navier–Stokes equations on structured multiblock grids. For each case, the focus is on the physics unveiled by the use of a localized LES resolution and how it improves the CFD prediction of quantities of interest for the engineer.

#### (a) Low-speed conditions

Among the aerodynamics issues raised by low-speed conditions, the prediction of the maximum lift and aeroacoustic sources remain the most challenging—yet some of the most critical—ones. The prediction of dynamic loads is also a topic of interest for slats/flaps installation and landing gear structural design. It is therefore necessary to simulate accurately the intimacy of the turbulent processes over realistic, complex geometries to understand the physics of the stall processes and determine the location and intensities of noise sources and their complex interactions with solid surfaces. As an example, take-off conditions are typically dominated by engine noise, whereas in landing and approach configurations, high-lift devices such as slats and flaps and landing gear have been identified as dominant sources of airframe noise [25–28]. The use of hybrid RANS–LES simulations to improve CFD predictions of aerodynamic performance and noise of the latter configurations is illustrated in this section.

The flow over a three-element aerofoil is inherently complex and exhibits a wide range of physical phenomena including large low-speed areas, strong pressure gradients, confluence of

boundary layers and wakes as well as unsteadiness and three-dimensionality on fairly large scales. The existence of different flow regions induces conflicting demands on the grid. As an example, the capture of the slat wake and its downstream evolution is of primary importance as regards to the evolution of the maximum lift coefficient. The computation of this wake in LES mode and its evolution over the main wing would require extremely fine grids beyond affordability. Hence, ZDES permits one to limit the focus regions to the slat and flap coves as well as to the flow field over the flap (see discussions in [19,29,30]).

This modelling technique has been assessed on the LEISA three-element aerofoil designed by DLR [31]. The zonal strategy retained and the modes used for this simulation are depicted in the upper part of figure 4. One can note that mode 1 of ZDES is retained in the slat and flap coves (problem of category I; figure 3) whereas mode 2 is used on the upper side of the flap where the location of separation is not known *a priori*. The turbulent content of the boundary layer is rebuilt close to the main wing trailing edge, thanks to mode 3 of ZDES.

The salient features of the instantaneous flow field in the slat and flap regions are highlighted in the middle part of figure 4. The flow in the slat cove displays a large recirculation bubble bounded by a shear layer emanating from the slat cusp and reattaching near the slat trailing edge. Figure 4 clearly illustrates the roll-up of two-dimensional eddies in the shear layer that rapidly develop spanwise deformations that amplify with downstream distance. The break-up of spanwise rollers into more random structures characterizes the transition of the mixing layer to a fully developed turbulent regime. Just before the shear layer impingement on the wall, the eddies experience a strong deformation owing to the highly accelerated slat gap flow. The flap cove flow has many similar features to the leading-edge slat flow. The three-dimensional organization of the wake flow is evidenced. The states of the different flow regions are related to one another and an unsteady analysis allows one to obtain more insights into the flow physics and to identify acoustic sources.

As an example, in the lower part of figure 4 showing the instantaneous dilatation field, both sound waves and turbulent flow regions are evidenced along with pressure spectra computed within the slat and flap cavities and in the inviscid region away from the wing. Three epicentres of approximately circular wave patterns can be identified at the trailing edges of the slat, main wing and flap. On the numerical side, it is also worth noting that the LES content in the wing boundary layer is quickly regenerated without introducing spurious acoustic contamination at the RANS–LES interface. This issue is of major importance when dealing with aeroacoustics calculations.

Back to the physical aspects, figure 4 also displays the sound pressure levels (SPLs) for points located in the slat and flap coves as well as in the outer field, respectively. Tonal components at low frequency emerge from the broadband content as well as from the high-frequency narrowband noise induced by the different trailing edge (TE) wakes. Of interest, it has been shown in [29] that a large-scale coupled self-sustained oscillation mechanism between slat and flap cavities, evidenced by spectral analysis, occurs at a Strouhal number  $St = 3\text{--}6$  based on the main wing chord and free-stream velocity. This yields an acoustic feedback mechanism characterized by a normalized frequency depending on the free-stream Mach number and the main wing chord like  $St = (1 - M_0^2)/2M_0$ . This result suggests that this coupled self-sustained oscillation mechanism involving both cavities may lead to a more intense sound in the framework of an ideal two-dimensional three-element aerofoil.

Along with the noise generated by high-lift devices as explained above, the flow around landing gear is another important source of noise for an aircraft in landing configuration [26]. However, if CFD-based noise predictions have reached a fairly good level of confidence for jet noise, then considerable efforts have been pursued recently to increase the reliability of CFD predictions of airframe noise, and especially of landing gear (representative configurations have been selected as common test cases for the AIAA Workshop on Benchmark Problems for Airframe Noise Computations, since 2010 [32]). The issue at stake is to be able to compute the far-field noise radiated by landing gear. This means that one has to accurately compute both the near-field noise sources (turbulent separations close to the landing gear, free shear

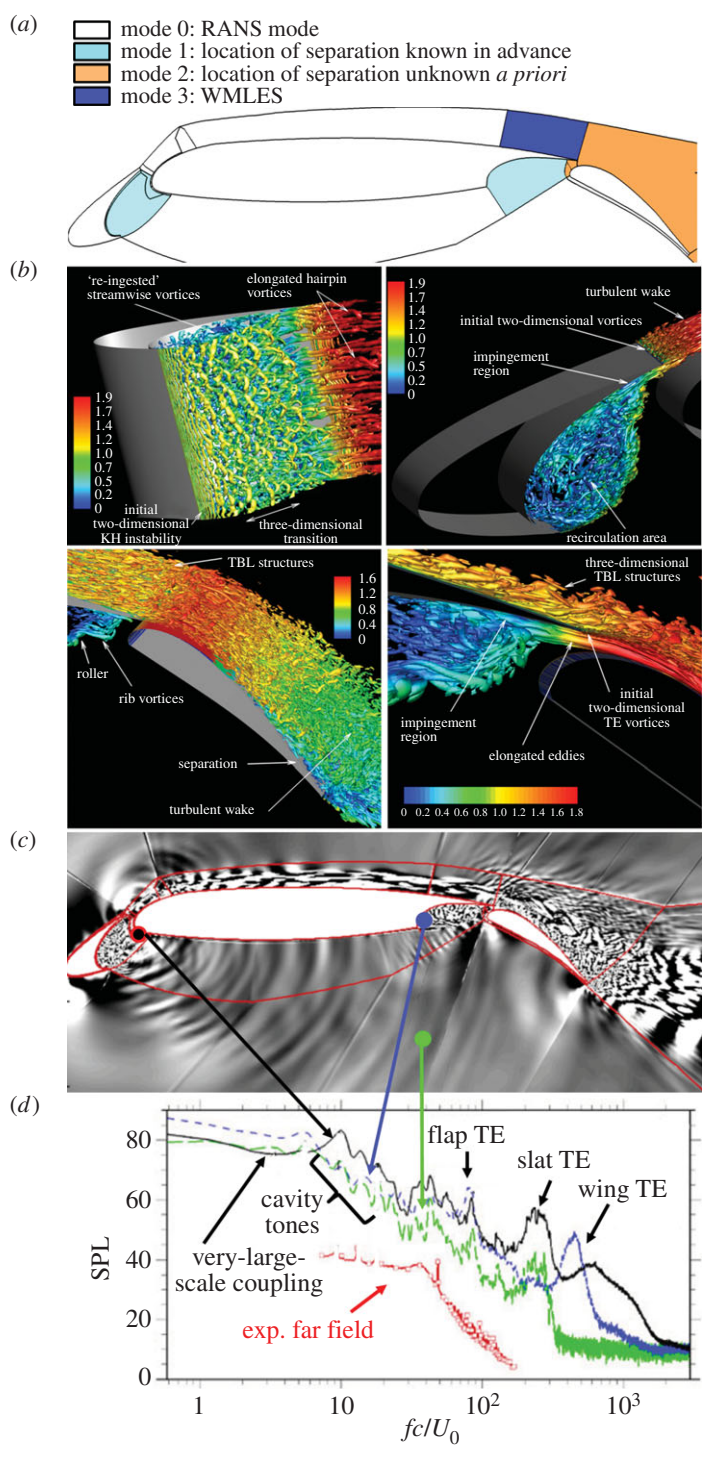


**Figure 4.** (a) ZDES of a three-element aerofoil ( $Re_{AMC} = 2 \times 10^6$ ,  $M = 0.15$ ,  $48 \times 10^6$  points). Modes 1, 2 and 3 are used as described in the picture. (b) Q-criterion isosurface shaded (coloured online) by the normalized streamwise velocity  $U/U_\infty$  highlighting the turbulent eddies in the slat cove and the flap. (c) Instantaneous field of  $(1/\rho)\partial\rho/\partial t$  highlighting the acoustic waves. (d) Sound pressure levels (SPLs) in the slat, flap and far-field areas. Adapted from Deck & Larauie [29]. (Online version in colour.)



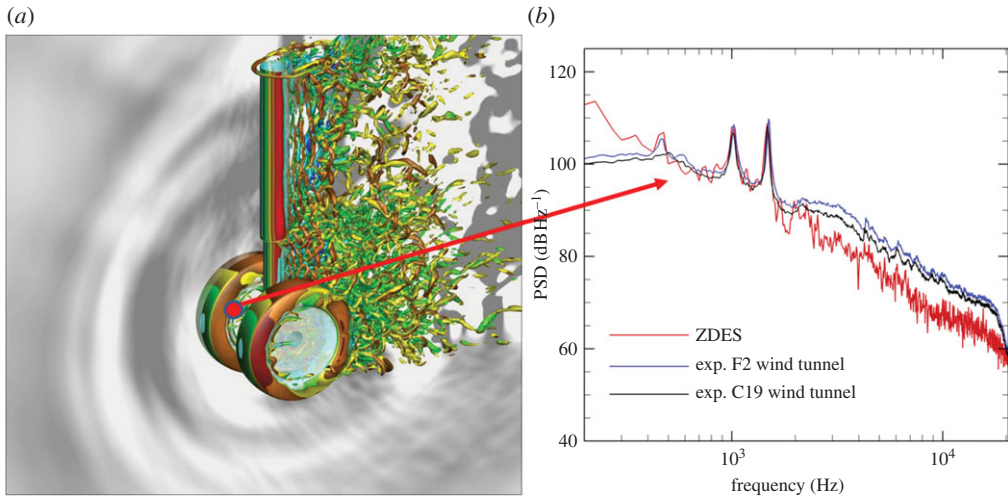


**Figure 5.** ZDES of the flow around a simplified landing gear ( $Re_{\text{diameter}} = 1.5 \times 10^6$ ,  $M = 0.23$ ,  $35 \times 10^6$  points). Mode 1 is used in the separated areas, mode 0 is used everywhere else. (a) Instantaneous pressure fluctuation field (black and white) which indicates that the main noise source may be located near the wheels and Q-criterion isosurface shaded (coloured online) by the streamwise velocity component showing the extent of the turbulent resolved field. (b) Sound pressure spectrum of pressure fluctuations on the wheel exhibiting a broadband shape with tonal peaks associated with wheel cavity resonance. (Online version in colour.)

layers impinging wall boundaries, vortex shedding) and the propagation of the generated noise to the ground, which involves totally different physics and relates to computational aeroacoustics (CAA). In this article, the focus is on the former issue, namely the simulation of aerodynamic noise sources, which also entails managing the geometric complexity, because flow separations and wake interactions between the geometrical details (struts, joints, dressings) of real-scale landing gear contribute significantly to the generated noise. Overset grids (or chimaera approach) seems to be a way to overcome this issue, even in the framework of RANS–LES methods [33,34].

To assess the reliability and maturity of the ZDES for such problems, the LAGOON [35] configuration has been computed and used as source data for CAA computations in [36]. The baseline geometry of the LAGOON landing gear configuration is a two-wheel nose landing gear (NLG) with simplified shapes. The overall dimensions of this model correspond to an A320 Airbus aircraft NLG at scale 1:2.5. This type of flow falls into the first category defined in figure 3, thus mode 1 is used in the separated areas and mode 0 (RANS mode) is used for the attached boundary layers upstream from the sharp edges that trigger separations. Of interest, it can be noted that this strategy allows the prescription of a laminar area to match the transition line used during the experiments, which is of major importance for CFD validation.

The features of the instantaneous flow field around the landing gear are depicted in figure 5. The flow is characterized by turbulent boundary layer separation, unsteady vortex shedding and intensive unsteady inter-element interaction. One can note that there is no delay in the formation of instabilities in the mixing layer. This is a major feature of mode 1 of the ZDES for which the length scale has been tailored to allow the fastest switch from RANS to LES. Besides, the pressure fluctuations around the landing gear shown in figure 5a indicate that the main noise source is roughly spherical and located in the area of the wheels.

The spectrum of pressure fluctuations for a sensor located on the internal side of the right wheel is plotted in figure 5b. This broadband spectrum also displays two fine tonal peaks at 1 and 1.5 kHz, which are most probably due to acoustic resonance effects of the cylindrical cavities at

the internal side of the wheels. The resonance is excited by the unsteady shear layers, which are accurately captured by the ZDES, comparing fairly well with experimental data. The broadband part of the noise is generated by turbulent flow separations and interactions between landing gear elements. In addition, this aerodynamic simulation was rather successfully used to allow the prediction of the far-field noise using the Ffowcs Williams and Hawkings (FW-H) porous surface integral method (unsteady data have been stored over surfaces enclosing the turbulent area (1 Terabyte), see [36]).

Because noise prediction and reduction are among the main objectives for simulations of low-speed configurations, it is important to note that the range of Strouhal numbers accessible by CFD-CAA simulations should be increased. The maximum frequency that can be resolved is limited by the mesh spacing, and most of the time, acoustic frequencies above a few kilohertz cannot be captured accurately. This limitation is mostly attributed to current CPU capabilities but it is a crucial issue since high-frequency noise sources (more than 10 kHz) can be observed in three-dimensional high-lift configurations for instance [26]. On the other hand, the most sensitive range of human noise perception lies between 0.5 and 3 kHz [26], which is achievable using present CFD-CAA capabilities.

## (b) Cruise conditions

As mentioned in the Introduction, CFD predictions for cruise conditions can also benefit from the use of advanced unsteady simulations. For instance, the interactions between the engine and the airframe are becoming all the more critical since high-bypass-ratio engines—which are more efficient—are considered. The consequences of these increased interactions are thermal and fatigue problems on the pylon and more complex noise source generations and reflections. Therefore, the correct simulation of the shear layer development and mixing is of primary importance to study these interactions. Indeed, the correct CFD prediction of pressure fluctuations on the pylon caused by the fan jet can help to reduce local panel fatigue leading to maintenance issues. Furthermore, the core jet turbulence coming from the combustion chamber and other upstream parts of the engine strongly impacts the mixing layers at the nozzle exit and modifies the jet development. Although sustaining free turbulence within a RANS computation remains somewhat challenging, the use of synthetic turbulence generation at the engine exhausts to account for this effect is straightforward with any eddy-resolving simulation.

The ZDES simulation of a realistic power plant installation has been performed [37,38] and is illustrated in figure 6. Mode 2 of the ZDES is applied inside the primary and secondary exhaust channels and close to the pylon in the jet development region. The RANS treatment of the attached boundary layers in these areas permits one to obtain the right integral boundary layer quantities at the separation point, which is a necessary condition to obtain the correct dynamics of the shear layer in the LES zones downstream. Mode 1 is applied downstream from the nozzle exit to resolve the mixing layers and jet development, and mode 0 is used elsewhere.

The flow visualization provided in figure 6 shows that there is no delay in the formation of instabilities in the mixing layers, thanks to the use of mode 1. Especially within ZDES, there is no need to switch off the subgrid-scale model to simulate accurately jet flows conversely to zonal RANS/implicit large eddy simulation (ILES), which have also proven to be efficient in certain situations like jet flows [39–41] and base flows [42–44]. The interaction of these instabilities with the pylon is captured by the simulation. Dynamic loads and temperature fluctuations can be quantified and their origin can be tracked to improve future designs.

Besides, one can see in the experimental measurements depicted in the bottom left of figure 6 that significant turbulence levels are observed in the primary and secondary jet cores. Therefore, a simple turbulent inflow generation based on stochastic harmonic functions was used to feed the ZDES simulation at the engine exit in order to match the turbulent content measured experimentally in both the primary and secondary exhausts. The synthetic turbulent structures injected are convected within the exhaust channels, taking advantage of

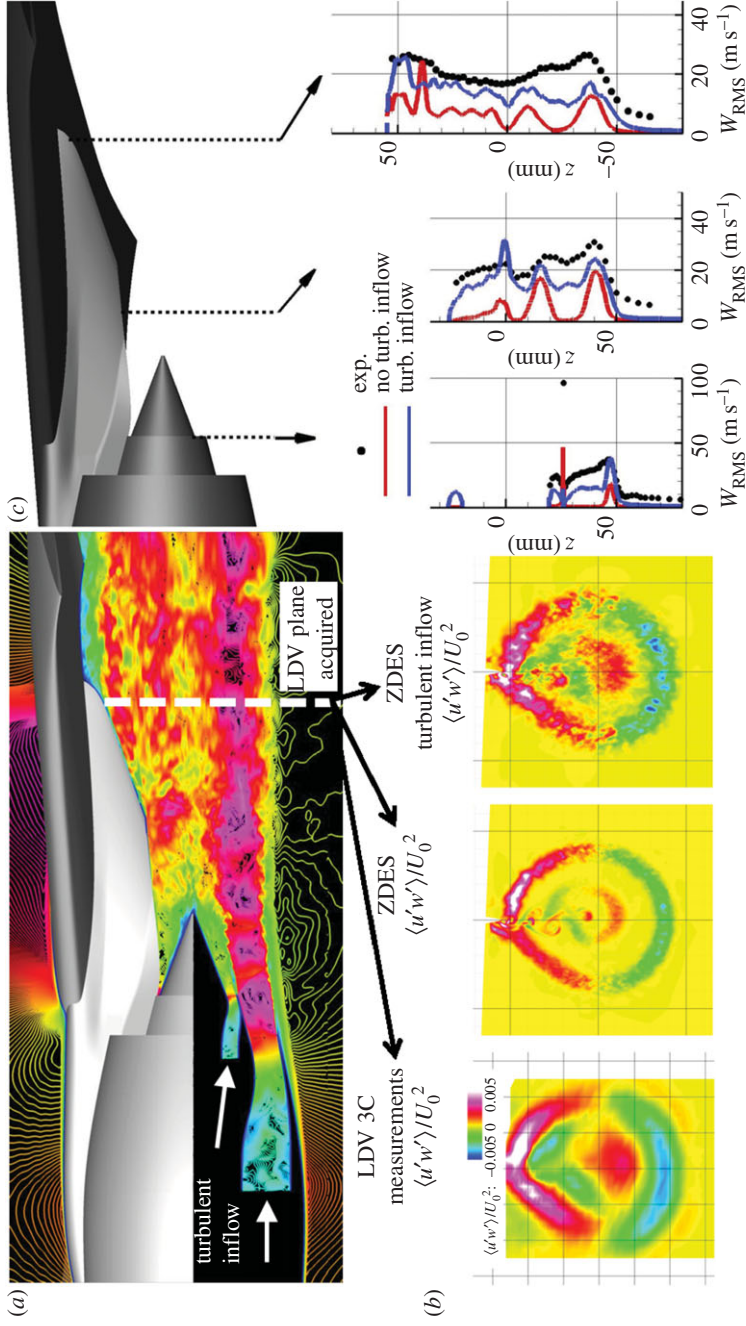


**Figure 6.** ZDES of the flow of a civil engine installation under a wing ( $Re_{AIC} = 1.5 \times 10^6$ ,  $175 \times 10^6$  points). Modes 1 and 2 are used. (a) Mach field in the engine axis highlighting the development of the shear layers and the jet mixing. (b) The  $\langle u'w' \rangle$  Reynolds stress. (c) The  $w_{RMS}$  velocity fluctuation profiles into the jet, emphasizing the necessity to use turbulent inflow generation at boundary conditions to reproduce the experimental conditions. Adapted from Brunet [38]. (Online version in colour.)

mode 2 of the ZDES to ensure a RANS treatment of the boundary layers in these areas while preserving the LES-like resolution of the turbulence in the core jets. Transverse velocity fluctuation profiles plotted in the right-hand side of figure 6 show that experimental levels of core turbulence can be matched by tuning the turbulent inflow method to the case considered. The comparison with the experiments also demonstrates the influence of the added turbulent inflow content on the shear layer development through a strong increase of the shear layer stress components.

### (c) Borders of the flight envelope

On the high-speed side of the flight envelope illustrated in figure 1, the buffet boundary draws a critical limit for aircraft, because structural fatigue, maintenance and passenger comfort are at stake. The status of ZDES predictions for two specific flight scenarios occurring at the borders of the flight envelope is commented on in this section: buffet onset and dive.

The transonic buffet is an aerodynamic phenomenon that results in a large-scale self-sustained motion of the shock over the surface of the aerofoil linked to the unstable nature of massive separation. For the sake of completeness, let us also mention the buffet on the horizontal tail plane of a civil aircraft, because, during flight, emergency descent situations are part of those extreme conditions that can lead the empennage of an airliner to vibrate [45]. These vibrations are mainly due to the separated flow on the upper surface of the structure, which increases the pressure fluctuations on the empennage, sometimes leading to buffet. The onset of this phenomenon is not related to any fluid–structure interaction, although it is inevitable that some structural vibrations—named ‘buffeting’—may result from the unsteady behaviour of the flow, which can lead to fatigue and cause structural damage. In these kinds of conditions, the physical challenges for CFD methods lie in the aerodynamic interaction on the wing between the shock, the incoming attached boundary layer upstream from the shock and the separation downstream from the shock. The inability of current CFD methods to predict buffet onset is such that, at the present time, buffet onset prevision and buffet characterization are based on many empiricisms and extensive use of wind tunnel and flight tests. Therefore, the very challenge for RANS–LES simulations is to provide direct access to the time and frequency distributions of the pressure fluctuations all over the wing, and especially around the shock location and in separated areas, to drive a significant increase in the quantitative CFD prediction of buffet onset, which is only accurately validated by aircraft makers in flight conditions at the present time.

The first ZDES of a transonic buffet configuration is analysed in [46] and more recent results on the same case are presented in figure 7. Of interest, for this specific case, the ZDES is used in an ‘automatic’ approach all over the suction side of the wing using mode 2, because the physical mechanisms involved are spatially evolving. Mode 2 of the ZDES allows the necessary dynamic location switch between RANS and LES domains to adapt the modelling level to the physics. Mode 0 is used for the fuselage and pressure side of the wing.

One can see in figure 7 the very complex three-dimensional interactions typical of buffet. As expected, the location of the switch between RANS and LES modelling follows the separated region dynamics, which allows a correct prediction of the integral boundary layer quantities upstream from the shock, because this area is treated in RANS mode. Besides, to ensure accurate comparisons with experiments, the transition line, the wind tunnel walls, the peniche and the measured model deformation are taken into account in the simulation. The simulation reproduces the shock motion, which is directly driven by the separation strength. This separation remains very close to the upper side of the wing, making the simulation even more challenging.

Results presented in figure 7 are in good agreement with wind tunnel tests even if the low-frequency fluctuations are slightly overestimated, which may be partly attributed to the short duration of the computed signal (typically 0.1 s) compared with the long-duration wind tunnel data (typically several seconds).

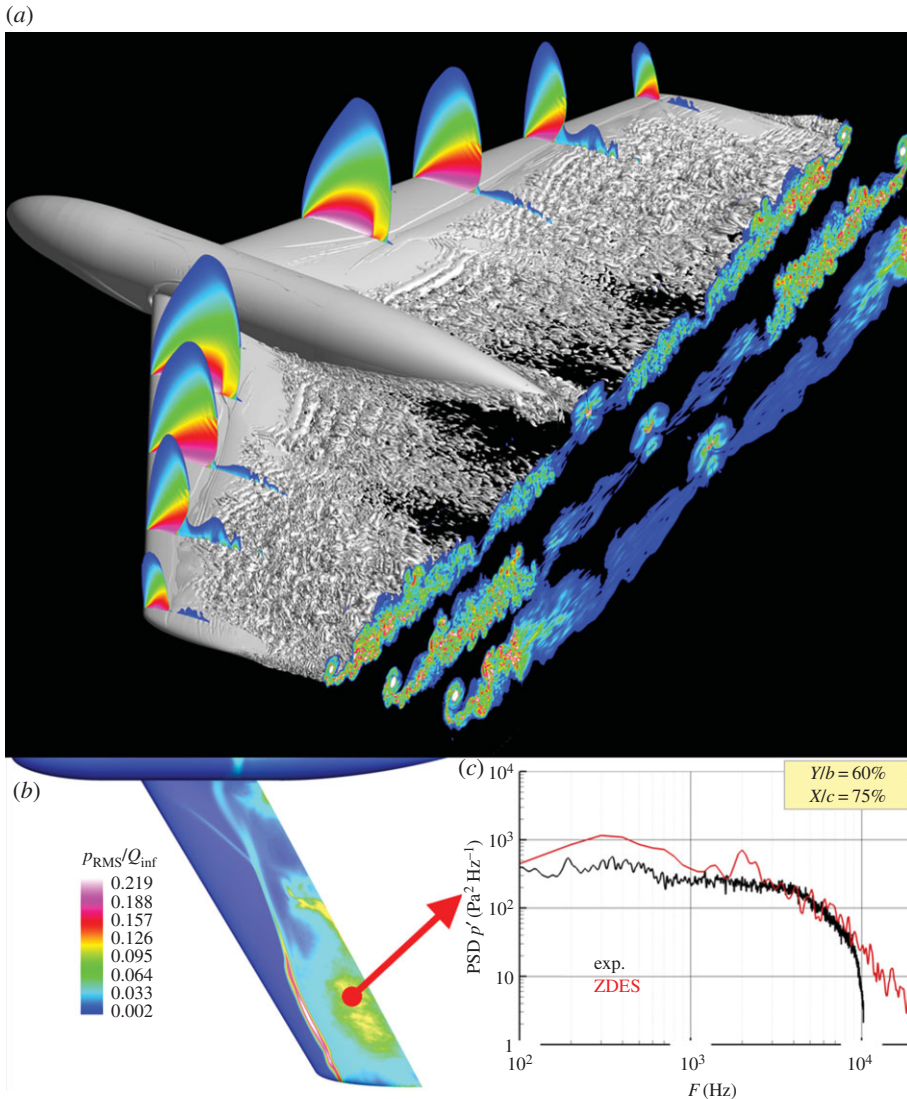


**Figure 7.** ZDES of transonic buffet over a civil aircraft configuration ( $Re_{AMC} = 2.8 \times 10^6$ ,  $M = 0.82$ ,  $190 \times 10^6$  points). Mode 2 is used for the whole wing suction side; mode 0 is retained on the fuselage and on the pressure side of the wing. (a) Isosurface of  $Q$ -criterion featuring the coherent structures resolved with ZDES mode 2 and vorticity and Mach contours. (b) Pressure RMS fluctuations on the suction side showing the location of the shock motion. (c) Pressure spectrum at the location identified in (b), within the separated area highlighting the broadband aspect characterizing the buffet on three-dimensional wings. (Online version in colour.)

Besides, it is noteworthy that the dynamic load studies allowed by this simulation require very long time signals in order to perform vibration studies since post-processing such as interspectra and phase previsions are necessary. Such signal analysis is not straightforward and relies on the use of advanced methods that necessitate long-duration datasets to achieve reliable results.

Another critical flight condition at the extremes of the flight envelope illustrated in figure 1 is the dive. This condition mostly impacts the certification and structural design of the aircraft. In particular, the prediction of the spoiler hinge moment is of major interest. Massive flow separations are created by spoilers to trigger the dive, which leads to an unsteady loading of the spoiler hinges that needs to be quantitatively assessed. At high Mach number, a shock-induced

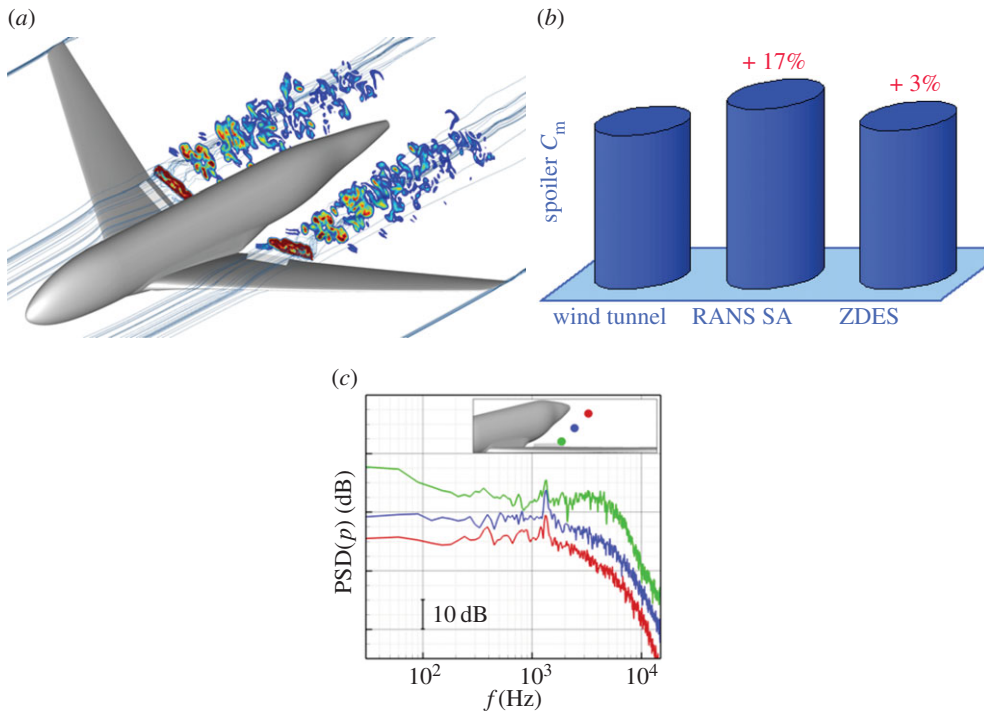


**Figure 8.** ZDES of an aircraft in dive conditions ( $Re_{AMC} = 5 \times 10^6$ ,  $M = 0.85$ ,  $40 \times 10^6$  points). Mode 1 is used downstream from the spoiler; mode 0 is used everywhere else. (a) Streamlines and vorticity contours show that turbulent content is resolved from the spoiler edges down to the aircraft tail. (b) Improvement of the spoiler hinge moment prediction with the time-averaged ZDES compared with experimental data and RANS Spalart–Allmaras simulation on the same grid. (c) Pressure spectrum in the spoiler wake underlines the presence of a tonal frequency in the wake far away from the spoiler. Adapted from Gand [47]. (Online version in colour.)

separation over the wing may exist and also interact with the spoiler. Besides, the wake of the spoiler has to be accurately resolved, as it may be impinging the horizontal tail and trigger tail buffet leading to handling issues in some cases.

The ZDES simulation of an aircraft in dive conditions has been performed [47] as illustrated in figure 8. Mode 1 was used to simulate the area downstream from the spoiler since the separation is triggered by the spoiler edge (figure 3). Everywhere else, mode 0 was retained since the flow is attached on the wing (no shock-induced separation upstream from the spoiler was observed during wind tunnel tests for this Mach number). To handle the geometrical complexity added by the spoiler deflected on the wing, the chimaera method has been used. This allows one to mesh independently the clean wing and the spoiler, which drastically reduces the user preprocessing load. This issue of handling geometrical complexity has already been pointed out for the landing gear application and is of major importance for the industrialization of hybrid RANS–LES simulations. This topic is further discussed in §4.

Figure 8 depicts typical results obtained in [47] which are significant in the framework of improving CFD confidence for flight conditions at the extremes of the flight envelope. In fact, one can see in figure 8b that the time-averaged value of the spoiler hinge moment is very well predicted by the ZDES. This result is attributed to the LES-like resolution of the unsteady turbulent separation and the mixing layer downstream of the spoiler edges with mode 1. Besides, figure 8(c) depicts the frequency distribution of the pressure fluctuations within the shear layer downstream of the spoiler, which indicates that a tonal excitation at somewhat high frequencies (around 1000 Hz at model scale) would have been impacting the horizontal tail plane of the model if it had been installed.

As a conclusion to the present section, it has been shown through several examples that ZDES simulations can have a significant added value in terms of accuracy and physical reliability for very different flow conditions all over the flight envelope depicted in figure 1. The presentation made in this section obviously cannot be exhaustive, and a number of relevant applications and critical flow problems have not been discussed, such as transitional flows, reattaching flows, moving control surfaces, jet noise, engine stall in crosswind, junction flows, etc. It can also be noted that other zonal RANS–LES methods are already commonly used in an R&T framework for aeroacoustic studies (which is one of the major issues for engine jets, for example to evaluate the influence of chevrons [39–41]), in low-speed conditions, and even in cruise conditions, as cabin noise has recently become a subject of primary importance to aircraft makers.

Nevertheless, a number of issues have been outlined regarding the maturity of RANS–LES for the simulation of technical configurations and the likelihood of actually using these approaches during the design cycle. These issues are further discussed in §4.

#### 4. Further discussion on remaining challenges and closing remarks

CFD is playing an expanding role in aerospace design, and enhancing its capabilities especially for unsteady flow simulations is considered as a major objective in the field. The understanding of flight physics, especially for nonlinear flows, can be a source of creativity aiming at new concepts. Furthermore, the ability to simulate accurately complex flows on realistic geometries allows the testing of innovative flow control strategies to reduce drag, noise, etc., which in the long run are all targeted at making aviation more environmentally friendly and also safer, more efficient and more economically viable in the context of strong competition between aircraft makers [48]. As an example, fuel is one of the largest operating expenses for an airline, and the fuel burn per seat is a particularly important parameter. Jameson & Fatica [49] indicate that an improvement of 5% in lift to drag ratio directly translates to a similar reduction in fuel consumption. Of interest, Jameson & Fatica [49] argue that a 5% saving of annual fuel cost of a long-range airliner (lying in the range \$5–10 million) would amount to a saving of \$10 million over a 25 year operating life. Besides, even a small performance advantage can lead to a significant shift of a very competitive market as suggested by Reneaux [50]: 1% drag reduction corresponds to a reduction of 1.6 tonnes on the operating empty weight or 10 passengers for a large civil aircraft—which still amounts to around 0.8 tonnes for a standard aircraft. Beyond these financial aspects, the former examples also show that, if the aircraft mass can be reduced thanks to a better prediction of aerodynamic loads, a significant reduction of drag and fuel consumption reduction can be achieved and therefore less gas emissions are produced by the aircraft.

This is why in the preliminary design stage, it is necessary to predict very finely the loads over the entire flight envelope. Towards these completely physics-based CFD simulations, it has been illustrated and argued in §3 that hybrid RANS–LES can be regarded as a viable and relevant solution. Among all the hybrid RANS–LES methods available, one may wonder which is the best approach. There is objectively no answer to this question and the only thing one can expect is to obtain an optimal combination of hybrid model, numerical method and grid for one specific flow. Eventually, useful results for design and understanding of civil aircraft aerodynamics can be obtained by adapting the level of modelling to the considered problem without waiting for the next generation of supercomputers.

As a response to the discussion on the zonal/non-zonal treatment of turbulence, each application presented in §3 relies on a different zonal strategy (operating possibly in an ‘automatic’ mode as in the buffet case). This observation supports the authors’ opinion that a universal method for industrial unsteady flows will not be available in the near future. The use of a zonal treatment of turbulence is therefore clearly advocated by the authors, because it provides an efficient framework to simulate accurately complex situations. Among this family of advanced methods, the ZDES method [15] is based on a fluid problem-dependent zonalization.

The ability of the latter method to handle technical applications relevant to civil aircraft aerodynamics is supported by a fair set of representative applications detailed in §3 showing

that the recent developments in hybrid RANS–LES are natural candidates for engineering applications. In particular, in the authors' opinion, modes 1 and 2 of the ZDES have proved to be accurate and robust enough to treat any flow configuration involving massively separated areas. Of interest, the delay in the formation of instabilities for such flows is no longer considered an issue with ZDES modes 1 and 2, as highlighted several times throughout the present article.

Actually, the limiting factor for the use of hybrid RANS–LES approaches in an industrial framework mainly lies in the capability to accurately handle geometrically complex configurations with validated unsteady tools. Some studies presented previously rely on the use of the chimaera method, which is frequently used for RANS computations but still needs to be thoroughly evaluated for unsteady approaches, because the interpolations between grid elements may dampen the instabilities resolved by physics-based simulations. Therefore, special care must be taken when building the overset grids to ensure that minimal interpolation error is made. Furthermore, CFD–CAA coupling simulations require high-order interpolations between overset grids to avoid filtering out the acoustic waves at chimaera overlaps. Other meshing techniques are being considered for RANS–LES simulations such as immersed boundary conditions and unstructured grids. This is a decisive issue, as aircraft makers are more and more interested in being able to predict local unsteady loads (for spoilers as presented above, but also for any air intake door, landing gear doors, etc.), which basically involve massively detached flows for which hybrid methods are mature enough to provide quantitative data that could help to reduce structural tolerances.

The challenge of handling complex geometries relates not only to computing cost, but also to solution quality in terms of meshing and validation of the computed unsteady field. In reference [51], it is emphasized that in the near future, if (really) complex configurations are considered, then the validation procedure should account for uncertainties and errors that arise from the very definition of the computational model and the post-processing of data of different nature. Accurate validation of system simulations will also require adequate experimental databases, which are still missing. Efficient tools to analyse large CFD dataset results are also essential.

The versatility of ZDES lies in its capability to be used not only in an industrial framework as argued above, but also for academic research. Among the next foreseen challenges in applied numerical aerodynamics, one may cite the capture of the boundary layer dynamics including transition and pressure-gradient-driven separation issues. As a typical example, the prediction of maximum lift of the aircraft, which is a limiting factor in take-off and landing performance, not only requires geometrical fidelity but relies heavily on the ability to detect the onset and extent of flow separation. This issue relates to the physics of the flow prior or close to separation, which is treated by RANS models within current RANS–LES approaches. More physics-based modelling needs to be available for such conditions. This is the purpose of the development of mode 3 of the ZDES—or WMLES in general—aimed at solving the outer part of the boundary layer (which still represents 90% of its thickness) and modelling the inner layer by a URANS approach to cope with these issues of smooth separation onset, which are of major interest to predict aircraft performance near stall.

Another physics-related challenge for RANS–LES methods is the understanding of high-Reynolds-number turbulent boundary layer dynamics, which not only covers a wide scope of practical applications in various domains of aeronautics, but also is an active field of research (figure 9). Many recent experimental results have suggested that the trend towards high Reynolds numbers could reveal some fundamentally different mechanisms at work in the dynamics of high-Reynolds-number boundary layers compared with their lower-Reynolds-number counterparts (see the reviews by Jiménez [53] and Smits *et al.* [54]). Hutchins & Marusic [55] emphasized the occurrence of large structures whose size can reach up to 15 boundary layer thicknesses long. They are called very-large-scale motions (VLSM) or superstructures. The role played by these structures in the boundary layer dynamics is still unclear, but Deck *et al.* [11,52] have recently emphasized how significant the contribution of the VLSM to mean wall shear stress is. The computational cost of a WRLES (or quasi-DNS) is extremely expensive because of the very small



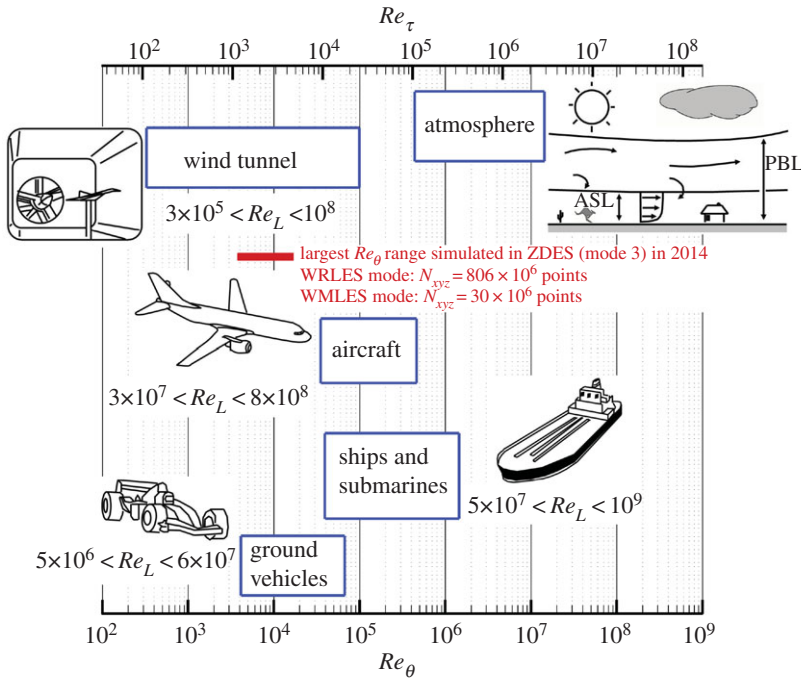


**Figure 9.** Typical Reynolds numbers in boundary layer applications.  $Re_L$  and  $Re_\theta$  denote the Reynolds numbers based on the streamwise characteristic length and momentum thickness, respectively.  $Re_\tau$  denotes the friction Reynolds number. ASL, atmospheric surface layer; PBL, planetary boundary layer. The largest wall turbulence simulation performed with ZDES (both in WMLES [11] and in WRLES [52] operating modes) in 2014 is emphasized along with the corresponding grid size. Note that the Reynolds number range achieved corresponds to the one commonly observed in subscale wind tunnels and that the use of WMLES allows a CPU cost reduction factor close to 30 compared with a complete WRLES simulation. Adapted from Deck *et al.* [52]. (Online version in colour.)

structures to be resolved in the inner layer, so that the benefit from the LES approach is quite reduced in the case of wall turbulence. In order to achieve a significant cost reduction, the near-wall dynamics has to be modelled while only the outer layer, i.e. 90% of the boundary thickness, is resolved. The development of WMLES strategies is a necessity to remove the prohibitive WRLES grid requirements of near-wall turbulence in high-Reynolds-number turbulent flows as encountered in aeronautical applications. This leads to computational costs that are within reach even for high Reynolds numbers (i.e.  $Re_\theta > 10^4$  typically encountered for wind tunnel subscale tests; figure 9). Consequently, the ability to simulate wall turbulence at high Reynolds number embedded in a curvilinear geometry (typically a swept wing or a fuselage to compute boundary layer noise, or for localized phenomena near vents and hatches, etc.) by limiting the spurious acoustics induced by classical synthetic turbulence methods is definitely one of the next challenges of advanced turbulence approaches.

In the end, from the aircraft makers' point of view, transferring the improved prediction capabilities of hybrid methods into the design cycle of aircraft is part of a process that will lead to the development of a complete numerical flight testing capability. Of course, this kind of capability relies on a wide multidisciplinary platform managing the interactions between aerodynamics and structures, acoustics, heat transfer, combustion, etc., which is far beyond the scope of the present article, which focuses on aerodynamics issues solely. The key improvement brought about by hybrid simulations would then be the ability to take into account nonlinearities of the flow at the early stages of the design cycle. It has been pointed out that, to reach this state of use of advanced unsteady methods, the stakes are as challenging as handling complex geometries,

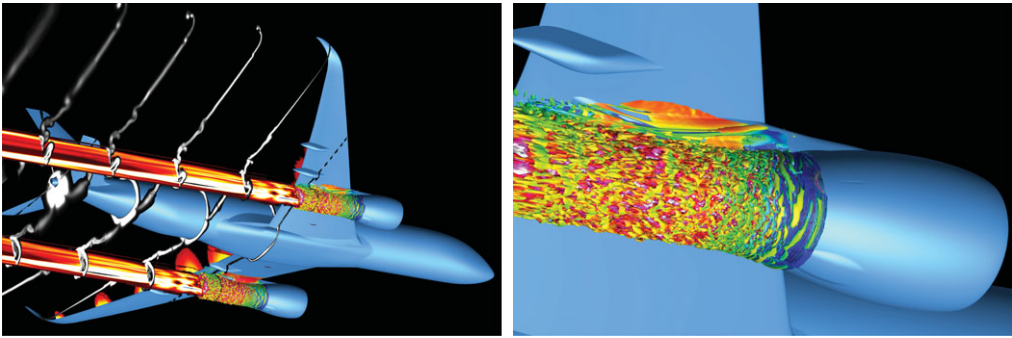


**Figure 10.** ZDES of the flow around a complete aircraft at scale 1 : 1 in true flight conditions, with focus on the jet development ( $Re_{AMC} = 50 \times 10^6$ ,  $M = 0.8$ ,  $200 \times 10^6$  points). Mode 2 is used for the whole computational domain. The grid size has been limited to  $200 \times 10^6$  points, thanks to the chimaera technique, which allows the use of a fine mesh only where it is necessary, namely in the jet development area. (Online version in colour.)

improving accuracy and robustness, validating and verifying the CFD results at the borders of the flight envelope, quantitatively predicting separation onset and modelling high-Reynolds-number wall turbulence.

It is important to note at this point that one of the next challenges for the use of hybrid methods lies in the training of aircraft designers in the use of such methods. Because each eddy-resolving simulation is likely to be devoted to solve a specific flow problem, it needs to be set up specifically to this effect and, even if all designers are not supposed be RANS–LES experts, advanced CFD methods require some additional knowledge that is not necessarily expected from RANS users. Defining general guidelines and procedures to ensure that RANS–LES methods are properly used is still an open issue (some hints are given for example in references [8,56]), but this educative process seems all the more essential, because the authors believe that an efficient, reliable, fully ‘automatic’ (i.e. non-zonal) and integrated RANS–LES formulation is beyond sensible expectations.

As argued in the beginning of the present section, the whole point of using hybrid RANS–LES at early design stages is for designers to be able to reduce tolerances by increasing the confidence level in CFD results, which in turn will lead to lighter, more fuel-efficient, thus greener, aircraft. This approach is not completely disconnected from economic issues, which cannot—and should not—be overshadowed. In fact, even if RANS–LES simulation turnaround time is still somewhat prohibitive in an industrial context, it is expected that progress in computer sciences and the growth of exacomputing and HPC will allow drastic development lead time reductions [12]. CFD will take advantage of every future increase in computer power and will increasingly compete with (and complete) flight tests, not just with wind tunnels. An example is provided in figure 10 where a complete aircraft at full scale 1 : 1 in true flight conditions ( $Re_{AMC} = 50 \times 10^6$ ) is simulated with a focus on the jet flow for an affordable CPU cost, because the grid size could be limited to  $200 \times 10^6$  points, thanks to the skillful combination of ZDES together with the chimaera technique.

As a conclusion, let us emphasize that RANS is still in high demand for aircraft design (among others) and for a long time to come. Hence, the true question is for which subsystems (i.e. subdomains) or flight conditions (like the border of the flight envelope) should we use advanced eddy-resolving methods to enable better decision making? This shows that RANS–LES methods will therefore remain a pacing item in aerospace engineering and a research subject.

**Funding statement.** The dive configuration simulation was carried out in the framework of European Project Aerodynamic Loads Estimation at the Extremes of the Flight Envelope (ALEF) supported by the Seventh Framework Programme of the European Commission (grant agreement number ACP7-GA-2009-211785). The computation of the three-element aerofoil was performed partly in the framework of the European GARTEUR

AG49 project with CIRA, DLR, EADS-M, FOI, INTA, NLR, ONERA and TUM as AG members. Part of the development and validation of the ZDES formulation was performed within the EU collaborative research project ATAAC (contract no. ACPS-GA-2009-233710-ATAAC), supported by the European Community in the Seventh Framework Programme. The power plant and buffet simulations were performed in the framework of national supported projects supported by the DGA and DGAC French agencies. The LAGOON project supported by Airbus France involves DLR, ONERA and Southampton University. The simulation of transonic buffet over a civil aircraft also benefited from HPC resources from GENCI-TGCC (grant no. t2010026310).

## References

1. European Commission. 2011 *Flightpath 2050, Europe's vision for aviation*. Technical report. Luxembourg, Belgium: Publications Office of the European Union. See <http://ec.europa.eu/transport/modes/air/doc/flightpath2050.pdf/>. (doi:10.2777/50266)
2. Green JE. 2003 Civil aviation and the environmental challenge. *Aeronaut. J.* **107**, 281–299. See <http://aerosociety.com/News/Publications/Aero-Journal/Online/328/Civil-Aviation-the-environmental-challenge/>.
3. Abbas Bayoumi A, Becker K. 2011 An industrial view on numerical simulation for aircraft aerodynamic design. *J. Math. Indust.* **1**, 1–14. (doi:10.1186/2190-5983-1-10)
4. Moin P, Kim J. 1997 Tackling turbulence with supercomputers. *Sci. Am.* **276**, 62–68. (doi:10.1038/scientificamerican0197-62)
5. Chapman DR. 1979 Computational aerodynamics development and outlook. *AIAA J.* **17**, 1293–1313. (doi:10.2514/3.61311)
6. Spalart PR, Jou WH, Strelets M, Allmaras SR. 1998 Comments on the feasibility of LES for wings and on a hybrid RANS/LES approach. In *Proc. First AFSOR Int. Conf. on DNS/LES, Ruston, LA, 4–8 August 1997*, pp. 137–147. Columbus, OH: Greyden Press.
7. Choi H, Moin P. 2012 Grid-point requirements for large eddy simulation: Chapman's estimates revisited. *Phys. Fluids* **24**, 011702. (doi:10.1063/1.3676783)
8. Sagaut P, Deck S, Terracol M. 2013 *Multiscale and multiresolution approaches in turbulence: LES, DES and hybrid RANS/LES methods: applications and guidelines*, 2nd edn, p. 448. London, UK: Imperial College Press.
9. Spalart PR. 2000 Strategies for turbulence modelling and simulations. *Int. J. Heat Fluid Flow* **21**, 252–263. (doi:10.1016/S0142-727X(00)00007-2)
10. Piomelli U, Balaras E. 2002 Wall-layer models for large-eddy simulations. *Annu. Rev. Fluid Mech.* **34**, 348–374. (doi:10.1146/annurev.fluid.34.082901.144919)
11. Deck S, Renard N, Laraufie R, Sagaut P. 2014 Zonal detached eddy simulation (ZDES) of a spatially developing flat plate turbulent boundary layer over the Reynolds number range  $3150 < Re_\theta < 14000$ . *Phys. Fluids* **26**, 025116. (doi:10.1063/1.4866180)
12. Slotnick J, Khodadoust A, Alonso J, Darmofal D, Gropp W, Lurie E, Mavriplis D. 2013 CFD vision 2030 study: a path to revolutionary computational aerospace sciences. Technical report, NASA Langley Research Center, NASA/CR-2014-218178. See <http://ntrs.nasa.gov/archive/nasa/casi.ntrs.nasa.gov/20140003093.pdf/>.
13. Haase W, Braza M, Revell A. 2009 *DESider: a European effort on hybrid RANS-LES modelling*. Notes on Numerical Fluid Mechanics and Multidisciplinary Design, vol. 103. Berlin, Germany: Springer. (doi:10.1007/978-3-540-92773-0)
14. Tucker P. 2013 *Unsteady computational fluid dynamics in aeronautics*. Fluid Mechanics and Its Applications, vol. 104. Berlin, Germany: Springer. (doi:10.1007/978-94-007-7049-2)
15. Deck S. 2012 Recent improvements of the zonal detached eddy simulation (ZDES) formulation. *Theor. Comput. Fluid Dyn.* **26**, 523–550. (doi:10.1007/s00162-011-0240-z)
16. Deck S, Weiss PE, Pamiès M, Garnier E. 2011 Zonal detached eddy simulation of a spatially developing flat plate turbulent boundary layer. *Comput. Fluids* **48**, 1–15. (doi:10.1016/j.compfluid.2011.03.09)
17. Tucker PG. 2013 Trends in turbomachinery turbulence treatments. *Prog. Aerosp. Sci.* **63**, 1–32. (doi:10.1016/j.paerosci.2013.06.001)
18. Tyacke J, Tucker P, Jefferson-Loveday RJ, Vadlamani NR, Watson R, Naqavi I, Yang X. 2014 LES for turbines: methodologies, cost and future outlooks. *J. Turbomach.* **136**, 061009. (doi:10.1115/1.4025589)
19. Deck S. 2005 Zonal-detached eddy simulation of the flow around a high-lift configuration. *AIAA J.* **43**, 2372–2384. (doi:10.2514/1.16810)

20. Deck S. 2005 Numerical simulation of transonic buffet over a supercritical airfoil. *AIAA J.* **43**, 1556–1566. (doi:10.2514/1.9885)
21. Spalart PR, Deck S, Shur ML, Squires KD, Strelets M, Travin A. 2006 A new version of detached-eddy simulation, resistant to ambiguous grid densities. *Theor. Comput. Fluid Dyn.* **20**, 181–195. (doi:10.1007/s00162-006-0015-0)
22. Deck S. 2012 Advanced turbulence modeling for aeroacoustics sources calculations. Application of zonal detached eddy simulation (ZDES). In *Aircraft noise* (eds R Dénois, E Lecompte, E Kors, C Schram), VKI Lecture Series 2012–02. Brussels, Belgium: von Karman Institute for Fluid Dynamics.
23. Spalart PR, Bogue DR. 2003 The role of CFD in aerodynamics, off-design. *Aeronaut. J.* **107**, 1072. See <http://aerosociety.com/News/Publications/Aero-Journal/Online/299/The-role-of-CFD-in-aerodynamics-off-design/>.
24. Cambier L, Heib S, Plot S. 2013 The ONERA elsA CFD software: input from research and feedback from industry. *Mech. Indust.* **14**, 159–174. (doi:10.1051/meca/2013056)
25. Delfs J. 2012 Airframe noise. In *Aircraft noise* (eds R Dénois, E Lecompte, E Kors, C Schram), VKI Lecture Series 2012–02. Brussels, Belgium: von Karman Institute for Fluid Dynamics.
26. Dobrzynski W. 2010 Almost 40 years of airframe noise research: what did we achieve? *J. Aircr.* **47**, 353–367. (doi:10.2514/1.44457)
27. Stoker RW, Guo Y, Streett C, Burnside N. 2003 Airframe noise source locations of a 777 aircraft in flight and comparisons with past model scale tests. AIAA Paper 2003-3232.
28. Piet JF, Michel U, Bohnning P. 2002 Localization of the acoustic sources of the A340 with a large phased microphone array during flight tests. AIAA Paper 2002-2506.
29. Deck S, Larauie R. 2013 Numerical investigation of the flow dynamics past a three-element aerofoil. *J. Fluid Mech.* **732**, 401–444. (doi:10.1017/jfm.2013.363)
30. Terracol M, Deck S. 2012 Numerical investigation of the flow around a three-element high-lift airfoil using two zonal hybrid RANS/LES methods: ZDES and NLDE. In *Progress in Hybrid RANS-LES Modelling* (eds S Fu, W Haase, S-H Peng, D Schwamborn). Notes on Numerical Fluid Mechanics and Multidisciplinary Design, vol. 117, pp. 345–355. Berlin, Germany: Springer. (doi:10.1007/978-3-642-31818-4\_30)
31. Wild J, Pott-Pollenske M, Nagel B. 2006 An integrated design approach for low noise exposing high-lift devices. AIAA Paper 2006-2843.
32. AIAA Discussion Group on Benchmark Experiments and Computations for Airframe Noise. Workshop on Benchmark Problems for Airframe Noise Computations. See [https://info.aiaa.org/tac/ASG/FDTC/DG/BECAN\\_files\\_/BANCII.htm](https://info.aiaa.org/tac/ASG/FDTC/DG/BECAN_files_/BANCII.htm).
33. Hedges LS, Travin AK, Spalart PR. 2002 Detached-eddy simulations over a simplified landing gear. *J. Fluids Eng.* **124**, 413–423. (doi:10.1115/1.1471532)
34. Spalart PR, Shur M, Strelets M, Travin A. 2012 Sensitivity of landing-gear noise predictions by large-eddy simulation to numerics and resolution. In *50th AIAA Aerospace Sciences Meeting*. AIAA Paper 2012-1174.
35. Manoha E, Bulte J, Caruelle B. 2008 LAGOON: an experimental database for the validation of CFD/CAA methods for landing gear noise prediction. AIAA Paper 2008-2816.
36. Sanders L, Manoha E, Ben Khelil S, François C. 2011 LAGOON: CFD/CAA coupling for landing gear noise and comparison with experimental database. AIAA Paper 2011-2822.
37. Brunet V, Deck S. 2010 Zonal detached eddy simulation of a civil aircraft engine jet configuration. In *Progress in Hybrid RANS-LES Modelling* (eds S-H Peng, P. Doerffer, W Haase). Notes on Numerical Fluid Mechanics and Multidisciplinary Design, vol. 111, pp. 147–156. Berlin, Germany: Springer. (doi:10.1007/978-3-642-14168-3\_12)
38. Brunet V. 2012 Random flow generation technique for civil aircraft jet simulations with the ZDES approach. In *Progress in Hybrid RANS-LES Modelling* (eds S Fu, W Haase, S-H Peng, D Schwamborn). Notes on Numerical Fluid Mechanics and Multidisciplinary Design, vol. 117, pp. 193–204. Berlin, Germany: Springer. (doi:10.1007/978-3-642-31818-4\_17)
39. Tucker PG. 2004 Novel MILES computation for jet flows and noise. *Int. J. Heat Fluid Flow* **25**, 635–635. (doi:10.1016/j.ijheatfluidflow.2003.11.021)
40. Shur ML, Spalart PR, Strelets M. 2005 Noise prediction for increasingly complex jets. Part I: methods and tests. *Int. J. Aeroacoust.* **4**, 247–256. (doi:10.1260/1475472054771385)
41. Xia H, Tucker P, Eastwood S. 2009 Large eddy simulations of chevron jet flows with noise prediction. *Int. J. Heat Fluid Flow* **30**, 1067–1079. (doi:10.1016/j.ijheatfluidflow.2009.05.002)
42. Simon F, Deck S, Guillen Ph, Sagaut P. 2006 Reynolds averaged Navier–Stokes/large eddy simulations of supersonic base flow. *AIAA J.* **44**, 2578–2590. (doi:10.2514/1.21366)

43. Kawai S, Fujii K. 2005 Computational study of a supersonic base flow using hybrid turbulence methodology. *AIAA J.* **43**, 1265–1275. (doi:10.2514/1.13690)
44. Baurle RA, Tam CJ, Edwards JR, Hassan HA. 2003 Hybrid simulation approach for cavity flows: blending, algorithm, and boundary treatment issues. *AIAA J.* **41**, 1481–1480. (doi:10.2514/2.2129)
45. Calderon R, Aupoix B, Calmels B, David C. 2012 Modelling aerodynamics unsteady loads on the horizontal tail plane of a civil aircraft. *Appl. Mech. Mater.* **432**, 543–547. (doi:10.4028/www.scientific.net/AMM.232.543)
46. Brunet V, Deck S. 2008 Zonal detached eddy simulation of transonic buffet on a civil aircraft type configuration. In *Advances in Hybrid RANS-LES Modelling* (eds S-H Peng, W Haase). Notes on Numerical Fluid Mechanics and Multidisciplinary Design, vol. 97, pp. 182–191. Berlin Germany: Springer. (doi:10.1007/978-3-540-77815-8\_19)
47. Gand F. 2013 Zonal detached eddy simulation of a civil aircraft with a deflected spoiler. *AIAA J.* **51**, 697–706. (doi:10.2514/1.J052106)
48. Flottau J, Haria R. 2013 Airbus, Boeing fight over 747, A380 performance data. *Aviation Week*, 6 August 2013. See <http://aviationweek.com/commercial-aviation/airbus-boeing-fight-over-747-a380-performance-data/>.
49. Jameson A, Fatica M. 2006 Using computational fluid dynamics for aerodynamics. White paper, National Research Council Workshop on the Future of Supercomputing, Santa Fe, NM, 24–25 September 2003. See [http://aero-comlab.stanford.edu/fatica/papers/jameson\\_fatica\\_hpc.pdf/](http://aero-comlab.stanford.edu/fatica/papers/jameson_fatica_hpc.pdf/).
50. Reneaux J. 2004 Overview on drag reduction technologies for civil transport aircraft. In *European Congress on Computational Methods in Applied Sciences and Engineering (ECCOMAS), Jyväskylä, Finland, 24-28 July 2004* (eds S Korotov, E Oñate, J Périaux, P Neittaanmäki, T Rossi, D Knörzer). See [http://www.imamod.ru/~serge/arc/conf/ECCOMAS\\_2004/ECCOMAS\\_V2/proceedings/author/authorR.html/](http://www.imamod.ru/~serge/arc/conf/ECCOMAS_2004/ECCOMAS_V2/proceedings/author/authorR.html/).
51. Sagaut P, Deck S. 2009 Large eddy simulation for aerodynamics: status and perspectives. *Phil. Trans. R. Soc. A* **367**, 2849–2860 (doi:10.1098/rsta.2008.0269)
52. Deck S, Renard N, Laraufige R, Weiss PE. 2014 Large scale contribution to mean wall shear stress in high Reynolds number flat plate boundary layers up to  $Re_\theta = 13650$ . *J. Fluid Mech.* **743**, 202–248. (doi:10.1017/jfm.2013.629)
53. Jiménez J. 2012 Cascades in wall-bounded turbulence. *Annu. Rev. Fluid Mech.* **44**, 27–45. (doi:10.1146/annurev-fluid-120710-101039)
54. Smits AJ, McKeon BJ, Marusic I. 2011 High Reynolds number wall turbulence. *Annu. Rev. Fluid Mech.* **43**, 353–375. (doi:10.1146/annurev-fluid-122109-160753)
55. Hutchins N, Marusic I. 2007 Evidence of very long meandering features in the logarithmic region of turbulent boundary layers. *J. Fluid Mech.* **579**, 1–28. (doi:10.1017/S0022112006003946)
56. Spalart PR. 2001 Young-person’s guide to detached eddy simulation grids. Technical report, NASA Langley Research Center, NASA/CR-2001-211032. See <http://ntrs.nasa.gov/archive/nasa/casi.ntrs.nasa.gov/20010080473.pdf/>.